δ-Opiate DPDPE in Magnetically Oriented Phospholipid Micelles: Binding and Arrangement of Aromatic Pharmacophores

Frank Rinaldi,* Mengfen Lin,#§ Michael J. Shapiro,# and Matthew Petersheim*
*Chemistry Department, Seton Hall University, South Orange, New Jersey 07079, and #Department of Analytics, Core Technologies, Novartis Pharmaceuticals Corporation, 556 Morris Ave., Summit, New Jersey 07901

ABSTRACT D-Penicillamine^{2,5}-enkephalin (DPDPE) is a potent opioid peptide that exhibits a high selectivity for the δ-opiate receptors. This zwitterionic peptide has been shown, by pulsed-field gradient ^{1}H NMR diffusion studies, to have significant affinity for a zwitterionic phospholipid bilayer. The bilayer lipid is in the form of micelles composed of dihexanoylphosphatidylcholine (DHPC) and dimyristoylphosphatidylcholine (DMPC) mixtures, where the DMPC forms the bilayer structure. At high lipid concentration (25% w/w) these micelles orient in the magnetic field of an NMR spectrometer. The resulting ^{1}H-^{13}C dipolar couplings and chemical shift changes in the natural abundance ^{13}C resonances for the Tyr and Phe aromatic rings were used to characterize the orientations in the bilayer micelles of these two key pharmacophores.

INTRODUCTION

It has been proposed that some messenger peptides may first associate with the phospholipids of cell membranes before binding to their target receptor (Schwyzer, 1977; Gysin and Schwyzer, 1984; Sargent and Schwyzer, 1986). The local order provided by the lipid bilayer could impose conformational constraints on the normally flexible peptides and help arrange the recognition sites of the peptide for binding to the receptor. If this is true, then the arrangement of the peptide in the membrane should correlate with biological activity.

The opioid peptides represent a good basis set for testing this idea. There are at least three different types of opioid receptors, μ, δ and κ (Wingard et al., 1991; Herz, 1993), which appear to differ in the location of the binding site with respect to the membrane surface (Schwyzer, 1986). All three classes of opioids have an N-terminal phenolic group from tyrosine as one pharmacophore and a second aromatic pharmacophore, usually phenylalanine, that determines the receptor selectivity through its topological relation to the tyrosine (Tourwe et al., 1996). Furthermore, there are a large number of analogs that have been characterized in terms of potency and selectivity for the various receptors. What remains is to characterize the membrane-bound conformations of these peptides and determine whether there is a correlation with activity.

There are two general approaches in using NMR for studying peptide structure in membranes. One employs conventional high-resolution NMR methods to obtain nuclear Overhauser (NOE) measures of interatomic distances and three-bond scalar coupling for dihedral angles. Whereas these measurements are readily incorporated into molecular modeling studies, the observed NOEs and couplings are population-weighted averages of the free and bound conformers. These experiments usually involve isotropic micelles (Karslake et al., 1990; Wooley and Deber, 1987; Hicks et al., 1992; Graham et al., 1992) or small unilamellar lipid vesicles (SUVs) (Reynaud et al., 1993; Okada et al., 1994). Both of these systems exhibit significant surface curvature with lipid or surfactant packing that differs from the planar bilayer surface assumed for a normal phospholipid membrane. To obtain enough NOE and coupling measurements to model the peptide structure, this approach generally requires perdeuteration of the surfactant to avoid obscuring essential resonances.

The second general approach uses "solid-state" measures of functional group orientation in the bilayer, i.e., chemical shift anisotropy (CSA) or resonance splittings due to dipolar coupling or quadrupolar coupling. These phenomena arise only with the peptide bound to the membrane, somewhat alleviating the complication of averaging between free and bound states. In this second approach the membrane mimetic systems are usually composed of phospholipid bilayers that better represent a conventional cell membrane, at least in terms of surface curvature, headgroup composition, and headgroup packing. Suspensions of multilamellar liposomes exhibit CSA and the dipolar or quadrupolar couplings as broad Pake patterns (Murari et al., 1986; Bechinger et al., 1993; Hu et al., 1995; Lee et al., 1995; North et al., 1995), which suffer from poor resolution and sensitivity. The orientational information can be preserved while Pake patterns are collapsed to relatively sharp resonances, if the lipid is oriented in the magnetic field. This can be accomplished by using lipid-coated glass plates (Opella et al., 1994; Hu et al., 1995) or magnetically oriented micelles (Sanders and Prestegard, 1990, 1991; Sanders et al., 1993; Sanders, 1993; Henderson et al., 1994; Howard and Prestegard, 1995, 1996; Sanders and Landis, 1995, Howard and Prestegard, 1996; Prosser et al., 1996). The CSA then man-

Received for publication 6 June 1997 and in final form 18 September 1997.

Address reprint requests to Dr. Matthew Petersheim, Chemistry Department, Seton Hall University, South Orange, NJ 07079-2694. Tel.: 201-761-9029; Fax: 201-761-9772; E-mail: petersm@shu.edu or petersma@lanmail.shu.edu.

§ Dr. Mengfen Lin's current address is Central Research, Pfizer Inc., Eastern Point Rd., Groton, CT 06340.

0006-3495/97/12/3337/12 $2.00

ifests as changes in chemical shift and the couplings as resonance splittings.

Although ^{1}H-^{1}H dipolar couplings in these experiments could provide interatomic distances over a much longer range than NOE measurements, these long-range couplings in a ^{1}H-rich environment usually lead to resonance broadening and poor definition of the coupling patterns (Meiboom and Snyder, 1971). The lower gyromagnetic ratio of ^{13}C greatly reduces contributions from long-range couplings, as does the fact that carbon atoms are usually sterically less accessible than hydrogen atoms. Consequently, ^{1}H-^{13}C couplings are observed for directly bonded atoms and some vicinal sites, giving a simpler coupling pattern that is even less sensitive to the local environment than NOE measurements. Likewise, CSA and quadrupolar couplings reflect only the immediate electronic environment of the nucleus. These local phenomena do depend on the orientation of the particular interaction vectors with respect to the magnetic field, which is determined by how the species is bound to the ordered lipid. Molecular modeling with these observations as constraints requires that both molecular orientation in the bilayer as well as conformation satisfy the experimental data, whereas NOE and three-bond scalar coupling constraints deal with conformation alone. A general approach to performing the combined orientational and conformational searches has been developed by Prestegard, Sanders, and co-workers (Sanders and Prestegard, 1990, 1991, 1992; Howard and Prestegard, 1995). As with conventional NMR/modeling studies, complete structural analysis of the membrane-bound species requires observations from several different sites in the molecule. In either approach to membrane studies, this generally requires some type of isotopic enrichment in the species of interest or isotopic depletion in the lipid to obtain an adequate number of unique measurements.

Our immediate goal is to develop a simple method for establishing the relative arrangement of the opiate Tyr and Phe pharmacophores in phospholipid bilayers as a means for testing Schwyzer's hypothesis (Schwyzer, 1977; Gysin and Schwyzer, 1984; Sargent and Schwyzer, 1986). The choice of natural-abundance ^{13}C NMR represents a compromise in maximizing the structural information from the experiments while avoiding isotopic enrichment, so that the method can be readily applied to a large group of peptides at little expense. For our purposes it is sufficient to study only the aromatic resonances, with ^{13}C CSA and ^{1}H-^{13}C dipolar coupling as measures of ring orientation in the lipid. Magnetically oriented phospholipid micelles were chosen as the means for creating the anisotropy, because they are easy to handle and they give rise to relatively narrow resonances, preserving sensitivity and resolution. Our intention is to apply this approach to several active and inactive opioid peptides to determine whether the pharmacophore orientations correlate with activity.

The work presented here deals with characterizing the relative orientations of the Tyr and Phe pharmacophores for a synthetic δ-opiate analog, DPDPE (Tyr-cyclo-[D-Pen-Gly-Phe-D-Pen]), when it is bound to phospholipid micelles. This peptide was chosen because it is very potent and highly selective for δ-receptors, and the crystal structure is known (Mosberg et al., 1983; Flippen-Anderson et al., 1994). The solution structure has also been thoroughly studied by NMR and molecular modeling, revealing a high degree of conformational entropy in the 14-member cyclic backbone (Smith et al., 1991).

The DPDPE results are compared with similar studies of Met-enkephalin (Kimura et al., 1996) and two Met-enkephalin analogs (Kimura et al., 1997), the δ-active [D-Ala^2]- and inactive [L-Ala^2]-Met-enkephalins. In those studies a cesium perfluorooctanoate liquid crystal was used, structural studies were performed using ^{1}H-^{1}H dipolar couplings, and rotating-frame Overhauser effects measured from the magnetically oriented spectra, using two-dimensional magic-angle-spinning and near-magic-angle-spinning experiments.

MATERIALS AND METHODS

Materials

1,2-Dimyristoyl-sn-glycero-3-phosphocholine (DMPC) and 1,2-dihexanoyl-sn-glycero-3-phosphocholine (DHPC), both >99% purity, were purchased from Avanti Polar Lipids (Alabaster, AL). Disodium salt of 1,3-benzenedisulfonate (BDS), 80% purity, was obtained from Aldrich Chemical Co. (Milwaukee, WI). Deuterium oxide (D_2O) with a minimum isotopic purity of 99.9% and D-penicillamine^{2,5} enkephalin DPDPE (Tyr-cyclo-[D-Pen-Gly-Phe-D-Pen]), 99% purity, were purchased from Cambridge Isotope Labs (Woburn, MA) and Sigma Chemical Company (St. Louis, MO), respectively. The lipids and peptide were used without further purification.

Preparation of NMR samples

DHPC/DMPC micelles were prepared by adding stoichiometric amounts of each of the dry micelle components to a tared 5-mm NMR tube. A volume of 100 mM phosphate buffer, 100 mM NaCl, and 10 mM cacodylate at pH 6.5, uncorrected for the isotope effect, was subsequently added to the NMR tube. The mixture was then subjected to multiple cycles of heating (40°C), cooling (5°C), vortexing, and low-speed centrifuging (~400 rpm) until the sample was optically clear and oriented in the NMR magnetic field (Sanders and Prestegard, 1990). DPDPE was weighed with a Sartorius microgram balance, added directly to the NMR tube, and mixed until completely dissolved.

NMR spectroscopy

PFG ^{1}H NMR experiments were carried out on a Bruker DMX-400 NMR spectrometer equipped with an Acustar II field gradient accessory. Because oriented samples exhibit severe ^{1}H-^{1}H dipolar broadening, a DHPC/DMPC mole ratio of 1/1.5 (25% w/w phospholipid) was used for these ^{1}H experiments because it is just outside the range of compositions that orient. In a typical PFG NMR experiment, 22 spectra were collected as a function of gradient pulse strength at 40°C, using the LED pulse sequence (Gibbs and Johnson, 1991). The gradient pulse strength was varied from 0.03 Tm^{-1} to 0.43 Tm^{-1}. Spectra were processed with XWINNMR software, and the diffusion coefficient of the peptide was calculated by the SPLMOD method as described elsewhere (Morris and Johnson, 1993).

Experiments with magnetically oriented DMPC/DHPC samples were run on a General Electric QE 300 at 7.05 Tesla, running with a Tecmag

interface and using a General Electric 5-mm dual ^{1}H/^{13}C probe. All spectra were acquired on samples maintained at 40°C, well above the chain melting transition temperature of DMPC bilayers (Cevc and Marsh, 1987). The ^{13}C proton decoupled spectra were achieved with square-wave modulated broadband decoupling.

All of the experiments used for the assignments for DPDPE were performed on a Bruker 500 MHz model AMX500 NMR at 11.75 Tesla. The ^{1}H, COSY, HMQC (heteronuclear multiple quantum correlation spectroscopy), and HMBC (heteronuclear multiple bond correlation spectroscopy) experiments were run on nonspinning samples, using a 3-mm inverse detected probe, and the ^{13}C spectrum was acquired on a spinning sample with a 3-mm broad-band probe, both supplied by Nalorac. The ^{1}H spectrum was acquired by using a standard 1 pulse sequence with a ~60° pulse, 32 transients, a total recycle delay time of 3.9 s, 16K real and imaginary points, and a spectral width of 17.24 ppm. The ^{13}C spectrum represents 150K transients acquired by using a standard one-pulse sequence with continuous 1 W ^{1}H WALTZ modulated decoupling power with an ~60° carbon pulse width equal to 4 μs, a spectral width of 265 ppm, a total recycle delay of 2.3 s, 16K real and imaginary points zero filled to 32K real points, and 4 Hz exponential line broadening.

The COSY spectrum (Aue et al., 1976) was acquired using 1024 by 256 points in f2 and f1, respectively, with a square spectral window of 17.24 ppm, 4 dummy scans, 8 scans per record, a total recycle delay time of 3 s, and a ^{1}H 90° pulse width of 6.0 μs collected in magnitude mode. The data was Fourier transformed using a sine bell apodization function in both dimensions to produce a zero-filled 1024 by 1024 spectrum.

The HMQC spectrum was acquired using a standard Bruker BIRD pulse sequence (Bax and Subramanian, 1986) with GARP ^{13}C decoupling optimized for one bond ^{1}H-^{13}C correlations, a ^{1}H 90° pulse width of 6 μs, 32 transients, 4 dummy scans, a 3.35-ms evolution time, a 360-ms delay to give a null for ^{1}H-^{12}C coherences, a 17.24 by 200 ppm spectral width, and 1024 by 256 points in f2 and f1, respectively. The data was zero filled in f1 to produce a square 1024 point data set, which was Fourier transformed using a sine bell apodization function shifted by $\pi/2$ in both dimensions. The apparent signal-to-noise ratio of the spectrum was further improved by using power spectrum mode processing.

The HMBC spectrum was acquired by using a standard Bruker pulse sequence (Bax and Summers, 1986), which was optimized for three-bond ^{1}H-^{13}C correlations, with a low-pass J filter to suppress one-bond correlations, a ^{1}H 90° pulse width of 7.1 μs, 96 transients, 4 dummy scans, a 3.44-ms evolution time, a 70-ms delay for long-range coupling evolution, and a spectral width of 17.24 by 200 ppm, defined by 1024 by 256 points in f2 and f1, respectively. The data was zero-filled in f1 to produce a square 1024-point data set, which was Fourier transformed using a sine-bell apodization function shifted by $\pi/2$ in both dimensions. The apparent signal-to-noise ratio of the spectrum was further enhanced by processing in the power spectrum mode.

Theoretical expressions

Magnetic ordering of the micelles gives rise to anisotropic averaging of ^{1}H-^{13}C dipolar couplings and ^{13}C chemical shifts. Dipolar coupling between nuclei i and j (D_{ij}) for a peptide bound to oriented micelles can be analyzed as follows (Sanders and Prestegard, 1992; Howard and Prestegard, 1995):

$$D_{ij} = A_{ij} f S(3\langle\cos^2\alpha\rangle - 1)/2 \quad (1a)$$

$$A_{ij} = -\gamma_i\gamma_j h/(2\pi^2 r^3) \quad (1b)$$

where γ_i and γ_j are the gyromagnetic ratios of the interacting nuclei, h is Planck's constant, and r is the internuclear distance between i and j, which yield an A_{ij} of -46.6 kHz for ^{1}H-^{13}C interaction at a bond length of 0.108 nm (Weast, 1983). The other terms are the fraction of DPDPE bound to the micelle, f, and the micelle order parameter, S. This last term accounts for the direction of the bilayer normal with respect to the field, which ideally is 90° in these studies, and "wobble" in the ordering of the micelles. The number of geometrically independent observables available in these experiments is insufficient (vide infra) for the order matrix approach (Sanders and Prestegard, 1990, 1992). Consequently, the angle, α, is between the interaction vector, that is the C-H bond, and an axially symmetric molecular director (D_b), presumably normal to the bilayer surface. The geometric definition of D_b is found in Fig. 1 *A*.

In an analogous fashion, the chemical shift anisotoropy (CSA) can be described as follows (Howard and Prestegard, 1995):

$$\delta_{or} = (1-f)\delta_{aq} + f\{\delta_{iso} + (2/3)S[\Delta_{12}(3\langle\cos^2\alpha_1\rangle - 1)/2 + \Delta_{32}(3\langle\cos^2\alpha_3\rangle - 1)/2]\} \quad (2)$$

$$\Delta_{ab} = \sigma_{aa} - \sigma_{bb}$$

where δ_{or} is the ^{13}C chemical shift of DPDPE in the presence of oriented micelles, δ_{aq} is that for peptide free in solution, δ_{iso} is that for peptide bound to the lipid but isotropically averaged, and the terms weighted by S are the shift due to magnetic ordering. The positions of the tensor components with respect to the DPDPE aromatic rings are taken as shown in Fig. 1 *B*, with σ_{33} parallel with the C-H bond, σ_{11} perpendicular to the ring, and σ_{22} perpendicular to both σ_{11} and σ_{33} (Pausak et al., 1974); α_1 and α_3 are the angles between D_b and the σ_{11} and σ_{33} vectors, respectively.

The goal of this work is to characterize the conformation of DPDPE when it is bound to the phospholipid bilayer. As a matter of convenience, we have chosen the DPDPE aromatic rings as local frames of reference, with the z axis normal to the ring and the x axis along the γ-β carbon-carbon bond. Our model of the aromatic ring assumes that it is a perfect planar hexagon. The orientation of the individual rings is described in terms of the orientation of D_b within the frame of the ring, that is, the cos(α) terms in Eqs. 1 and 2 are expanded in terms of the corresponding spherical polar coordinates:

$$\cos\alpha_i = \sin\theta_i\cos\phi_i\sin\theta_D\cos\phi_D + \sin\theta_i\sin\phi_i\sin\theta_D\sin\phi_D + \cos\theta_i\cos\theta_D \quad (3)$$

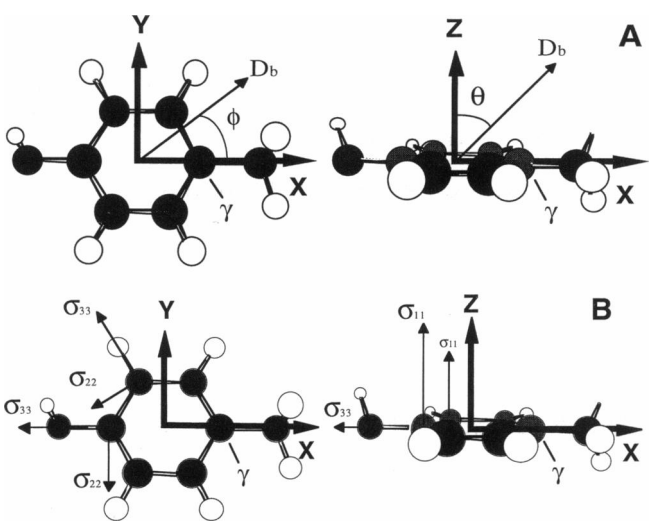

FIGURE 1 Coordinate system for the aromatic ring used in computations. (*A*) The molecular director, D_b, is defined with θ_D relative to the axis normal to the ring, and the projection of the director into the ring is at ϕ_D with respect to the C_γ-C_β bond. Carbons are shaded, and hydrogen is white. (*B*) The carbon shielding tensor has σ_{11} perpendicular to the plane of the ring and σ_{33} along the bonds directed out of the ring.

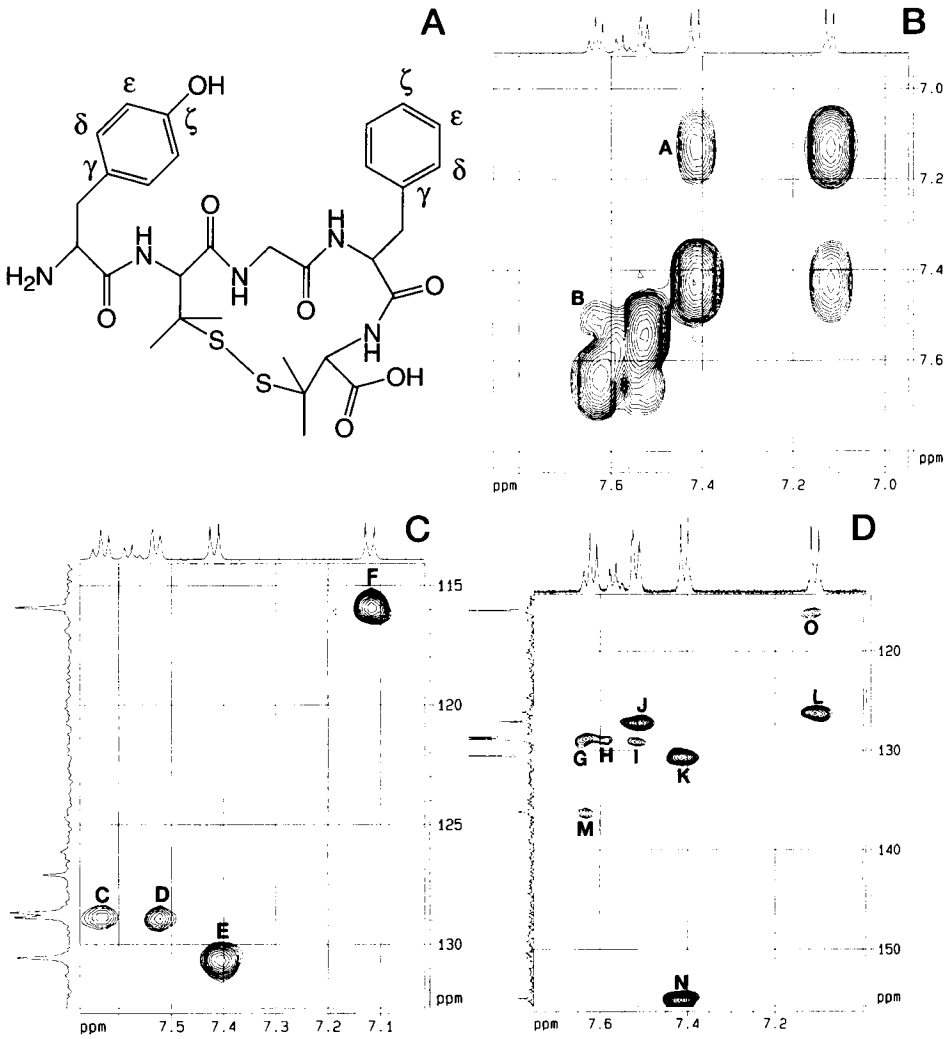

FIGURE 2 Resonance assignments for DPDPE in aqueous solution. (*A*) Atom labeling for the aromatic rings of DPDPE. (*B*) The COSY spectrum of 3.4 mM DPDPE in 100 mM phosphate, 100 mM NaCl, 10 mM cacodylate buffer at pH 6.5. COSY $^3J_{1H\text{-}1H}$ cross-peaks: A: Tyr-δ to Tyr-ϵ; B: Phe-δ to Phe-ϵ. (*C*) The HMQC spectrum of the same solution. HMQC $^1J_{1H\text{-}13C}$ cross-peaks: C: Phe-ϵ; D: Phe-δ; E: Tyr-δ; F: Tyr-ϵ. (*D*) The HMBC spectrum of the same solution. HMBC $^2J_{1H\text{-}13C}$ and $^3J_{1H\text{-}13C}$ cross-peaks: *G: Phe-ϵ_H to Phe-ϵ_C; H: Phe-ζ_H to Phe-δ_C; *I: Phe-δ_H to Phe-δ_C; J: Phe-δ_H to Phe-ζ_C; *K: Tyr-δ_H to Tyr-δ_C; L: Tyr-ϵ_H to Tyr-γ_C; M: Phe-ϵ_H to Phe-γ_C; N: Tyr-δ_H to Tyr-ζ_C; *O: Tyr-ϵ_H to Tyr-ϵ_C. *Some ^1J cross-peaks are detectable in the HMBC experiment, despite the use of low-pass J filtering to suppress one-bond correlations.

where θ_i, ϕ_i are the polar coordinates for the ith interaction vector and θ_D, ϕ_D are those for D_b. Taking into account the symmetry of both rings in the x-z plane, the interactions for the δ_1 and δ_2 carbons, and likewise for the ϵ_1 and ϵ_2 carbons, are direct averages:

$$\langle\cos^2\alpha_i\rangle = (\langle\cos^2\alpha_i\rangle_1 + \langle\cos^2\alpha_i\rangle_2)/2 \qquad (4)$$

where the subscript i refers to the particular interaction vector and the subscripts 1 and 2 outside the brackets refer to δ_1 and δ_2 carbons or the ϵ_1 and ϵ_2 carbons.

RESULTS

DPDPE solution NMR assignments

The solution spectra of DPDPE in a buffer of the same composition as that used in the DHPC/DMPC experiments was used to determine the aromatic proton and carbon resonance assignments. Resonance assignments were performed by a scheme that mutually satisfies the COSY, HMQC, and HMBC spectra (Fig. 2). The assignments in the presence of DHPC/DMPC given in Table 2 are consistent with the solution assignments given in the caption of Fig. 2.

DPDPE bound to magnetically oriented micelles: effects on ^{13}C spectra

The NMR spectra of DPDPE in the presence of phospholipid micelles exhibit only one set of resonances (Fig. 3), which is consistent with aqueous DPDPE in fast exchange with the micelle-bound state. Consequently, the NMR properties for the peptide are population-weighted averages of the bound and free values. The aromatic peptide resonances are the focus of these studies, because they are well resolved from lipid resonances under all conditions, and the relatively rigid rings provide good frames of reference with well-defined chemical shift anisotropies for the carbons. Fig. 4 shows both coupled and decoupled ^{13}C spectra of the aromatic resonances for DPDPE in the presence of unoriented and oriented micelles. Magnetic ordering of the micelles results in changes in chemical shift for the bound-state peptide and manifestation of a dipolar contribution to resonance splittings for spectra collected without ^1H decoupling.

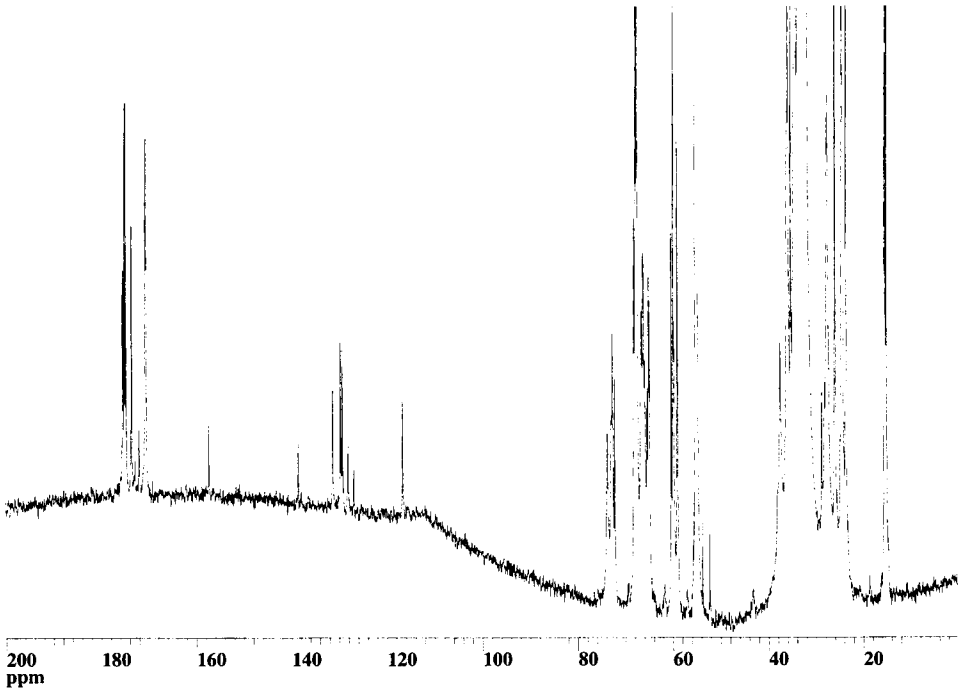

FIGURE 3 ^{1}H decoupled ^{13}C NMR spectra of 30.1 mM DPDPE in the presence of oriented DHPC/DMPC micelles (1/2.2 mole ratio) at 40°C. The high-intensity resonances from 15 to 80 ppm are from the phospholipid at high concentration (25% w/w), whereas the low-intensity resonances are primarily DPDPE. The carbonyls from phospholipid (*large peaks*) and DPDPE (*small peaks*) are visible from 170 to 180 ppm. The aromatic region from 110 to 160 ppm contains only DPDPE resonances. Note that only one set of DPDPE resonances is observed, indicating fast exchange between aqueous and micelle-bound states on the NMR time scale.

Estimating the micelle order parameter

The observed couplings and chemical shifts depend on the micelle order parameter, S, which has a value of $-1/2$ for micelles with the bilayer normal perfectly ordered perpendicular to the field. Sanders (1993) used the ^{31}P CSA of DMPC to measure S for these magnetically oriented micelles and established that S varies linearly with the ^{13}C chemical shift of the sn1-carbonyl resonance (CO1) according to

$$S = (-1/2)(\delta_{or} - \delta_{iso})/\Delta\delta \quad (5)$$

where δ_{or} and δ_{iso} are the chemical shifts of the CO1 resonance in the oriented and isotropic micelle system and $\Delta\delta$ is the shift difference expected for perfectly ordered micelles, which is equal to -9.2 ± 1.0 ppm (Sanders, 1993). Using this relation, S was found to be -0.22 for a DHPC/DMPC ratio of 1/2.2 and -0.35 for a ratio of 1/3.4.

PFG ^{1}H NMR diffusion measurements: fraction of DPDPE bound

Pulsed-field-gradient ^{1}H NMR diffusion experiments were used to estimate the fraction of the peptide bound to lipid micelles from the observed diffusion coefficient according to

$$D_{obs} = fD_{bound} + (1 - f)D_{free} \quad (6)$$

where D_{bound} is the diffusion coefficient of the peptide when bound to the micelles, which is the same as the diffusion coefficient of the micelles themselves. Rather than attempting to estimate the diffusion coefficient for the micelles, which are present as a distribution of sizes (Tausk et al., 1974), it was assumed that the micelles move significantly more slowly than the free peptide and that $fD_{bound} \ll (1 - f)D_{free}$. Therefore, the first term in Eq. 6 is neglected.

The self-diffusion coefficient obtained for 6.7 mM peptide at 40°C in the absence of the micelles (D_{aq}) is 21.0×10^{-6} cm^2/s. However, in the presence of a high concentration of lipid, the excluded volume generated by the micelles is expected to alter the diffusion of unbound peptide. To correct for this excluded volume, a species found to have little affinity for the micelles, benzenedisulfonate (BDS), was measured along with DPDPE, both in the presence and absence of micelles. The diffusion coefficient of BDS in buffer was 31.0×10^{-6} cm^2/s and 7.0×10^{-6} cm^2/s in the presence of the micelles. Assuming that the diffusion of unbound DPDPE scales in the same way as that of BDS, D_{free} for the peptide in the presence of the micelles is then 4.85×10^{-6} cm^2/s. In the presence of micelles, D_{obs} for the peptide under these conditions (DHPC/DMPC = 1/1.5; 25% w/w lipid; 40°C) is 3.0×10^{-6} cm^2/s. Using these values with Eq. 6, f is 0.40.

Separating scalar and dipolar coupling

The observed ^{1}H splitting of the ^{13}C resonances in the oriented spectra can be treated to first order as a sum of the scalar coupling present in the unoriented spectra and a term dependent on orientation, which is assumed to be solely dipolar coupling. In this case the two terms have opposite signs, because the magnitudes of the ^{1}H-^{13}C couplings were found to decrease in going from an isotropic sample to one with a low degree of ordering (data not shown). Table 1 lists the observed ^{1}H-^{13}C splittings and estimates of the dipolar contributions for DPDPE bound to micelles composed of

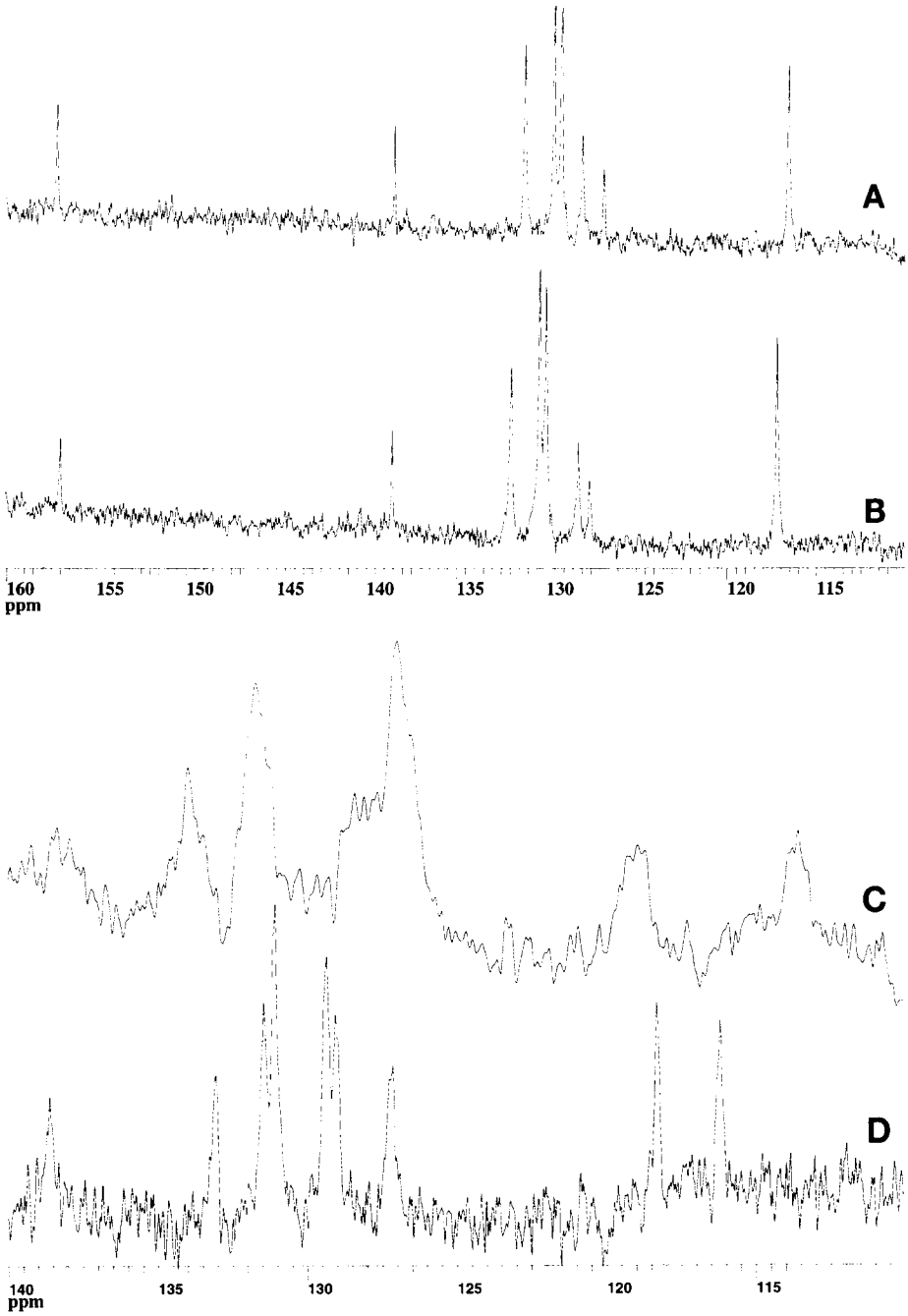

FIGURE 4 Aromatic region of the ^{13}C NMR spectrum of DPDPE in oriented and isotropic micelles. (*A*) ^{1}H decoupled ^{13}C spectrum of 30.1 mM DPDPE with oriented micelles (1/2.2 DHPC/DMPC, 25% w/w total lipid). (*B*) ^{1}H decoupled ^{13}C spectrum of 16 mM DPDPE with isotropic micelles (1/1 DHPC/DMPC, 25% w/w total lipid). (*C*) ^{1}H coupled ^{13}C spectrum of 30.1 mM DPDPE with oriented micelles (1/2.2 DHPC/DMPC, 25% w/w total lipid). (*D*) ^{1}H coupled ^{13}C spectrum of 16 mM DPDPE with isotropic micelles (1/1 DHPC/DMPC, 25% w/w total lipid).

1/1 DHPC/DMPC ($S = 0$), 1/2.2 DHPC/DMPC ($S = -0.22$) and 1/3.4 DHPC/DMPC ($S = -0.35$). Couplings for the Phe-ζ resonance were not resolved in these spectra.

Changes in chemical shift with lipid composition

Referencing the chemical shifts is complicated by the fact that any chemical shift standard added to the solution can partition between the aqueous and micelle phases. Consequently, the Tyr-ζ resonance in the oriented spectra was arbitrarily set to the same chemical shift assigned to it in the spectrum for the unoriented micelle sample (1/1 DHPC/DMPC). It also happens to be the most downfield aromatic resonance (Figs. 3 and 4). Chemical shifts for the other aromatic resonances are given in Table 2 for both isotropic and oriented micelle solutions. All three samples consisted of 25% total lipid by weight. Assuming that f is roughly the same for DHPC/DMPC ratios of 1/1 to 1/3.4, the change in chemical shift due to magnetic ordering ($\Delta\delta$) is given by the difference between the observed shift and that for the same resonance in the isotropic 1/1 DHPC/DMPC sample (Table 2).

According to Eq. 2, these $\Delta\delta$ should depend on f, S, and the orientation of the ring in the bilayer. The contribution

TABLE 1 ^{1}H-^{13}C couplings for DPDPE bound to isotropic and oriented micelles

DHPC*/DMPC	1/1	1/2.2		1/3.4	
	$S = 0^{\#}$	$S = 0.44^{\#}$		$S = 0.69^{\#}$	
Carbon	$\lvert J_{CH}\rvert$ Hz	$\lvert\Delta\nu_{CH}\rvert$ Hz	$\lvert D_{CH}\rvert^{\S}$ Hz	$\lvert\Delta\nu_{CH}\rvert$ Hz	$\lvert D_{CH}\rvert^{\S}$ Hz
Tyr-δ	147	420	567	622	769
Tyr-ε	158	408	566	622	780
Phe-δ	158	358	516	533	691
Phe-ε	160	360	520	535	695
Phe-ζ	164	—	—	—	—

*The mole ratio of DHPC to DMPC.
#Bilayer order parameter measured from the ^{13}C NMR spectrum of each sample, as described in the text.
§Absolute value of the dipolar coupling obtained from the observed resonance splitting, assuming the scalar coupling is of opposite sign.

from the ring orientation can be removed by taking the ratio of $\Delta\delta$'s for the two oriented samples, leaving only S_2f_2/S_1f_1. If it is assumed that f is the same for both samples, this ratio should equal S_2/S_1, which is 1.6 in this case. The Phe-γ, -δ, and -ϵ resonances are in good agreement with this value, the Tyr-δ and ϵ values are close, but the Tyr-γ and Phe-ζ are significantly lower than expected. Ratios of the dipolar couplings should also yield S_2/S_1. All of these ratios are close to 1.35 (Table 2), which is also lower than the expected value. These observations may be an indication that some of the peptide binds to the DHPC component of the micelle at low DMPC levels. To test this idea, attempts were made to work with micelles with significantly higher DMPC content, but they did not orient.

Ring orientations consistent with the observed dipolar couplings

Within the frame of reference for a given ring, all θ_i for the ^{1}H-^{13}C interaction vectors are 90°, and ϕ_i are ±60° and ±120° for δ and ϵ, respectively. Using these values and substituting Eq. 4 into Eq. 1 yields the following relation between the dipolar coupling and the orientation of the molecular director in that frame of reference:

$$D_{ij} = A_{ij}fS\langle[3\sin^2\theta_D(2\sin^2\phi_D + 1)/4 - 1]/2\rangle \quad (7)$$

Fig. 5 is a contour plot of $|D_{ij}|$ for ϕ_D versus θ_D, obtained using Eq. 7, with $f = 0.40$, $S = -0.22$, and $A_{ij} = -46.6$ kHz. The experimental values of $|D_{ij}|$ are 566 Hz for Tyr resonances and 518 Hz for Phe at $S = -0.22$ (Table 2), which are close to the lowest level contour shown that falls in the vicinity of $80° < \phi_D < 100°$ and $75° < \theta_D < 90°$. Very similar contours and results are obtained with the $S = -0.35$ data.

Relation between DPDPE ^{13}C chemical shift and its bilayer orientation

The chemical shifts of the resonances are easier to measure than the dipolar couplings, because they are obtained from decoupled spectra with sharper resonances and better signal-to-noise ratios. Equation 2 gives the relation between the chemical shifts and the orientation of the interaction vector in the micelles; however, it requires that the oriented and isotropic spectra have a reliable common reference. This issue of chemical shift reference was addressed in a previous section, with the Tyr-ζ resonance chosen as the reference for all micelle solutions (Table 2). Equation 2 then becomes

$$\begin{aligned}(\delta_j - \delta_k)_{or} - (\delta_j - \delta_k)_{iso} &= (1/3)Sf\{[\Delta_{12}(3\langle\cos^2\alpha_1\rangle - 1) + \Delta_{32}(3\langle\cos^2\alpha_3\rangle - 1)]_j \\ &\quad - [\Delta_{12}(3\langle\cos^2\alpha_1\rangle - 1\rangle + \Delta_{32}(3\langle\cos^2\alpha_3\rangle - 1)]_k\}/2 \\ &= \Delta\delta_{theor} \end{aligned} \quad (8)$$

where the subscript j is for the carbon of interest and subscript k refers to the Tyr-ζ carbon. Again, the cos α_i terms can be expressed in terms of the polar coordinates of the tensors and the director, by using Eq. 3; all $\theta_3 = 90°$, all

TABLE 2 ^{13}C chemical shifts for DPDPE with isotropic and oriented DHPC/DMPC micelles

DHPC*/DMPC	1/1 $S = 0$	1/2.2 $S = 0.44$		1/3.4 $S = 0.69$		$\Delta\delta(3.4)^{\S}/\Delta\delta(2.2)$	$\lvert D_{CH}(3.4)\rvert^{¶}/\lvert D_{CH}(2.2)\rvert$
Carbon	δ ppm	δ ppm	$\Delta\delta^{\#}$	δ ppm	$\Delta\delta^{\#}$		
Tyr-γ	127.65	126.71	−0.94	126.77	−0.88	0.94	
Tyr-δ	132.05	131.12	−0.93	130.71	−1.34	1.44	1.36
Tyr-ε	117.28	116.47	−0.81	116.11	−1.17	1.44	1.38
Tyr-ζ	157.11*	157.11*	0	157.11*	0	ND‖	ND‖
Phe-γ	138.66	138.36	−0.30	138.18	−0.48	1.60	
Phe-δ	130.46	129.50	−0.96	128.89	−1.57	1.63	1.34
Phe-ε	130.09	129.09	−1.00	128.45	−1.64	1.64	1.34
Phe-ζ	128.31	127.90	−0.41	127.80	−0.51	1.24	

*The chemical shift for all Tyr-ζ carbons has been set to 157.11 ppm (see text).
#$\Delta\delta_i = \delta_{or\,i} - \delta_{iso\,i}$, the difference between oriented and isotropic chemical shifts for carbon i.
§Ratio of $\Delta\delta_i$ at the higher DMPC content spectrum to that of the lower DMPC content spectrum.
¶Ratio of the absolute value of the C-H dipolar coupling of the higher DMPC content spectrum to that of the lower DMPC content spectrum.
‖ND, Not detected.

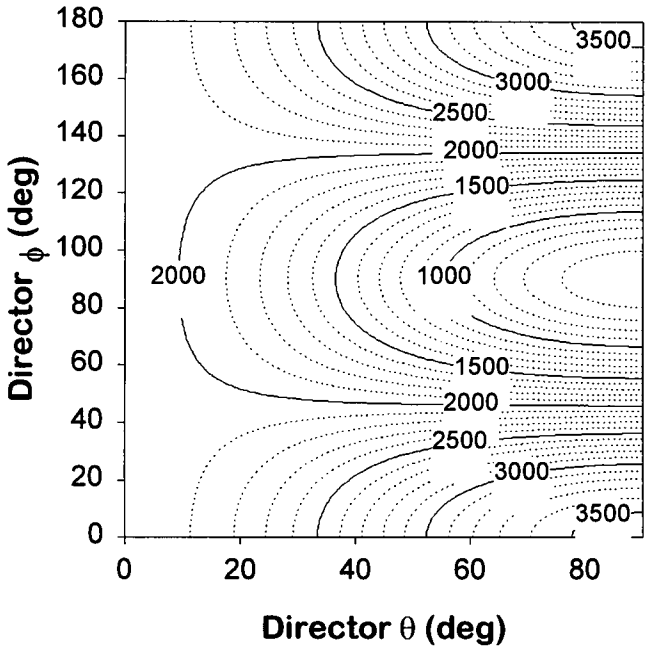

FIGURE 5 Contour plot of ^1H-^{13}C dipolar coupling magnitude, $|D_{ij}|$, as a function of the molecular director coordinates in the ring frame of reference. The dipolar coupling for the δ- and ϵ- aromatic resonances follows Eq. 7 in the text, where ϕ_D and θ_D are the polar coordinates of the molecular director defined in Fig. 1 *A*. The contours are for values of $|D_{ij}|$ in Hz, calculated using $A_{ij} = -46.6$ kHz, $f = 0.40$ and $S = -0.22$.

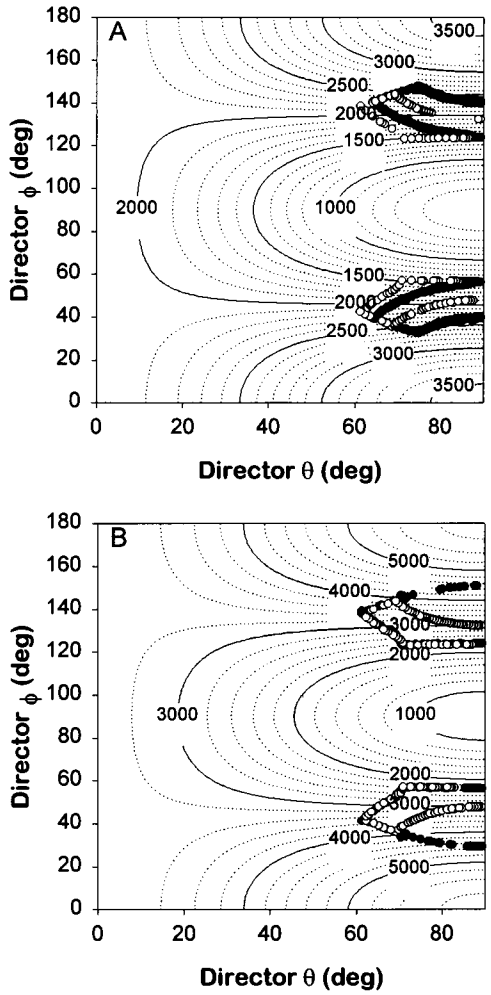

FIGURE 6 Director coordinates estimated from chemical shift changes overlaid on the $|D_{ij}|$ contours. Calculations for (*A*) $S = -0.22$ data and (*B*) $S = -0.34$ data. The symbols in both plots are for coordinates that gave predicted chemical shifts within 5% of the observed shifts for the Tyr (λ) aromatic resonances and the Phe (μ) aromatic resonances. Based on the overlap of chemical shift results with these contour plots, the experimental dipolar couplings are at least three times lower in magnitude than expected.

$\theta_1 = 0°$, and both ϕ_1 and ϕ_3 are 0°, ±60°, ±120°, and 180° for γ, δ, ϵ, and ζ carbons, respectively. A grid search of θ_D and ϕ_D values was performed, keeping those coordinates for which $\Delta\delta_{theor}$ is within 5% of the experimental $\Delta\delta$'s in Table 2. The carbon shielding tensors, $\{\sigma_{aa}\}$, used here are given in Table 3 and are values for C-H, C-O, and C-C averaged from several aromatic substances (Duncan, 1987). To take into account the uncertainty in these shielding values, the search was conducted by using minimum and maximum estimates of all Δ_{ik} values calculated from the average $\{\sigma_{aa}\}$ and their respective standard deviations.

Fig. 6, *A* ($S = -0.22$) and *B* ($S = -0.35$), display the results of this search superimposed on the $|D_{ij}|$ contours for both the Tyr (*filled circles*) and Phe (*open circles*) rings. The CSA data for each ring yields director coordinates in the range of $60° < \theta_D < 90°$, with $30° < \phi_D < 60°$ or $120° < \phi_D < 150°$. Note that the lowest $|D_{ij}|$ contours that overlap with the CSA results are for couplings of 1500 Hz with $S = -0.22$ (Fig. 6 *A*) and 2100 Hz with $S = -0.35$ (Fig. 6 *B*). These values of $|D_{ij}|$ are roughly a factor of 3 higher than the experimental values (Table 1). The simplest explanation for this discrepancy is that the CSA and the dipolar couplings are partially averaged by local fluctuations in the packing of the lipid molecules and the conformation of the bound peptide. All of the calculations presented above implicitly assume a rigid peptide and well-ordered lipids in the micelles. Partial averaging of the interactions due to local fluctuations could also account for the discrepancies among the $\Delta\delta(3.4)/\Delta\delta(2.2)$ and $|D_{CH}(3.4)|/|D_{CH}(2.2)|$ values in Table 2 (vide supra).

TABLE 3 Shielding tensor values used for the aromatic carbons (Duncan, 1987)

Carbon	σ_{11}* (ppm)	σ_{22} (ppm)	σ_{33} (ppm)	No. of spectra#
Tyr-δ, ε	215	145	17	24
Phe-δ, ε, ζ	(16)	(17)	(3)	
Tyr-γ & Phe-γ	221	160	21	18
	(11)	(9)	(9)	
Tyr-ζ	227	158	71	5
	(10)	(13)	(5)	

*The standard deviation is denoted parenthetically.
#The number of spectra used to generate the average σ_{ii}.

The two aromatic rings yield very similar plots of ϕ_D versus θ_D, suggesting that they have roughly the same orientations in the lipid bilayer. There are also only small differences in the plots for the 1/2.2 DHPC/DMPC and the 1/3.4 DHPC/DMPC data. Therefore, if DPDPE does bind to DHPC-rich regions and the DMPC bilayer, either the two sites orient the rings in a similar manner, or one of the sites dominates the results of these analyses.

Relative orientations of Tyr and Phe rings: membrane versus crystal structures

The director orientations computed above are defined with respect to the local coordinate system of the particular aromatic ring. If the Tyr and Phe rings have the same director (i.e., the peptide is conformationally constrained in the micelles), then the experimental CSA and dipolar couplings can be used to test proposed orientations of one ring relative to the other. The x-ray crystal structure of DPDPE exhibits three unique conformations per unit cell (Flippen-Anderson et al., 1994). To compare the Tyr and Phe rings, we have chosen to consider their relative dipolar couplings, which were found to be the same under all conditions, i.e., $|D_{CH}(\text{Tyr-}\delta)|/|D_{CH}(\text{Phe-}\delta)|$ and $|D_{CH}(\text{Tyr-}\epsilon)|/|D_{CH}(\text{Phe-}\epsilon)|$ are 1.1 for both DHPC/DMPC ratios. If the Phe ring is used to define the molecular frame of reference, then the denominator in these ratios is still Eq. 7. The Euler transformations needed to convert the crystal coordinates to the Phe ring frame are applied to the Tyr interaction vectors, giving a new set of coordinates, θ_i and ϕ_i, for Eq. 3. Consequently, the numerator in these ratios does not reduce to the simple form of Eq. 7 and varies with the particular conformation.

Fig. 7 shows computed values of $|D_{CH}(\text{Tyr})|/|D_{CH}(\text{Phe})|$ versus θ_D for the three different crystal conformations, MOL1 (*solid curve*), MOL2 (*dotted curve*), and MOL3 (*dashed curve*). There are generally two values of $|D_{CH}(\text{Tyr})|/|D_{CH}(\text{Phe})|$ for a given θ_D, corresponding to two possible values for ϕ_D. Note that the MOL1 and MOL3 conformations give good agreement with the experimental ratio of 1.1 (Fig. 7, *horizontal solid line*) near $\theta_D = 83°$ ($\phi_D = 29°$) and $\theta_D = 76°$ ($\phi_D = 29°$), respectively. Mol2 is never close to the experimental ratio. Fig. 8 depicts the MOL1 and MOL3 crystal structures, with the molecular director drawn through the rings to reflect these orientations. The Tyr phenolic group is presumably directed outward toward the aqueous phase, and the hydrophobic Phe ring is embedded deeper in the bilayer.

If the same coordinate transformations are applied to the Tyr shielding tensors, the predicted and observed chemical shifts for Tyr and Phe, again, show reasonable agreement with the MOL1 and MOL3 structures but not the MOL2 conformation. Using the chemical shifts observed at both 1/2.2 and 1/3.4 DHPC/DMPC, the two rings were in best agreement at $\theta_D = 69°$ ($\phi_D = 59°$) for MOL1 and $\theta_D = 80°$ ($\phi_D = 120°$) for MOL3.

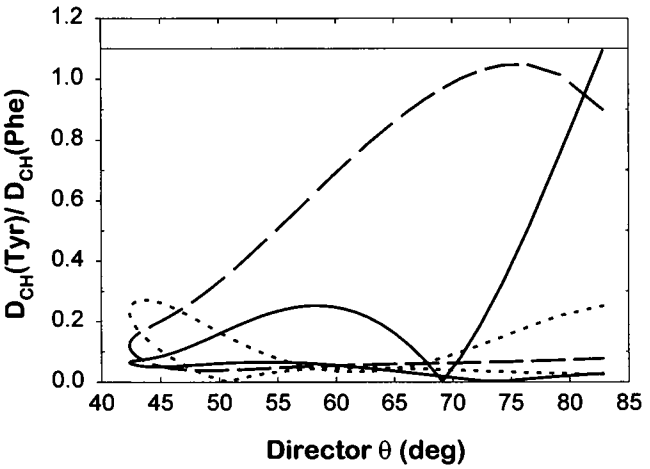

FIGURE 7 Relative dipolar couplings, $D_{ch}(\text{Tyr})/D_{CH}(\text{Phe})$, computed from the crystal coordinates for DPDPE. The ratio of Tyr-ϵ/Phe-ϵ and Tyr-δ/Phe-δ experimental dipolar couplings is 1.1 (*horizontal solid line*) for both 1/2.2 and 1/3.4 DHPC/DMPC. Plots of $D_{ch}(\text{Tyr})/D_{CH}(\text{Phe})$ were computed from the crystal coordinates (Flippen-Anderson et al., 1994) as a function of θ_D and ϕ_D in the Phe frame of reference. Results are given for all three conformers in the crystal: MOL1 (*solid curve*), MOL2 (*dotted curve*) and MOL3 (*dashed curve*). MOL1 (*solid curve*) and MOL3 (*dashed curve*) show good agreement with the experimental ratio of 1.1 (*horizontal solid line*) near $\theta_D = 83°$ ($\phi_D = 29°$) and $\theta_D = 76°$ ($\phi_D = 29°$), respectively. The MOL2 (*dotted curve*) has no orientation that yields the relative dipolar couplings observed in the experiments.

DISCUSSION

Given the amphiphilic nature of most biologically active peptides, it is very likely that many of them will have some affinity for phospholipid membranes. Binding of the peptide to membranes may be important in establishing the correct peptide-receptor interactions (Sargent and Schwyzer, 1986; Schwyzer, 1986), or may simply play a role in transport and bioavailability. To test the former, it will be necessary to characterize the membrane-bound conformations of a large number of active and inactive species. The purpose of the ^{13}C experiments presented here was to demonstrate a method for characterizing the arrangement of peptide pharmacophores that would be amenable to the study of a large collection of analogs.

PFG-diffusion studies show that ~40% of the DPDPE is bound to the unoriented phospholipid micelles in these experiments. Therefore, it is at least reasonable for this potent δ-opiate to associate with the membrane phospholipids in preparation for binding to the receptor, as proposed by Schwyzer (Sargent and Schwyzer, 1986). The activity of this and most other opioid peptides presumably depends on the arrangement of two aromatic pharmacophores (Schiller, 1984; Herz, 1993), the Tyr and Phe rings in the case of DPDPE. In the natural-abundance ^{13}C spectra, the aromatic resonances remain conveniently well resolved from all lipid resonances, even at 25% lipid (w/w). Most other resonances are either obscured or are more ambiguous in assignment as the micelles are oriented. Consequently, the analysis is limited to the chemical shifts of the Tyr and Phe aromatic

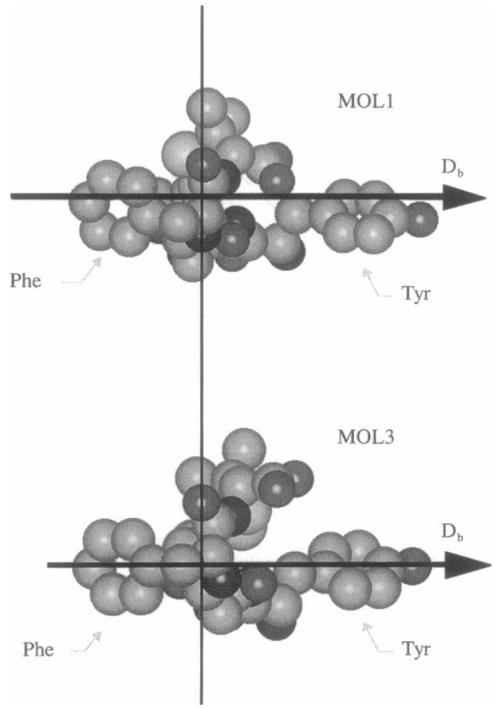

FIGURE 8 An adaptation of the x-ray crystal structure of hydrated DPDPE (Flippen-Anderson et al., 1994). The reported crystal structure contains three DPDPE molecules per unit cell, designated in this paper as MOL1, MOL2, and MOL3. Depictions of MOL1 and MOL3 are shown, with D_b oriented with respect to the Tyr and Phe aromatic rings, in agreement with the NMR CSA and ^1H-^{13}C dipolar coupling measurements. MOL2 did not show agreement with the NMR measured CSAs or ^1H-^{13}C dipolar couplings. The vertical line drawn through both figures is meant to represent the surface of the lipid bilayer.

carbons and ^1H-^{13}C dipolar couplings of those carbons on the rings with directly bonded hydrogens. The plane of symmetry running through the γ and ζ carbons results in the two δ-carbons being equivalent, and, likewise, the equivalence of the two ϵ-carbons. In addition, the ring is nearly a regular hexagon, which makes the δ-carbons geometrically equivalent to the ϵ-carbons. Because of these symmetries, there are not enough unique observables to define the full-order matrix (Sanders and Prestegard, 1991, 1992), and certainly not enough information to warrant the use of the combined ^1H-^{13}C dipolar couplings and ^{13}C chemical shift changes as constraints in modeling the whole molecule.

Our analysis focuses specifically on the arrangement of the Tyr and Phe aromatic pharmacophores, assuming an axially symmetric molecular director. In the first approach, the two rings were analyzed independently and were found to have very similar orientations in the phospholipid micelles, based on both the coupling and chemical shift data. However, the actual range of director coordinates predicted from the coupling data is offset from the coordinates calculated from the chemical shifts (Fig. 6). It is very likely that motions of the surrounding lipid molecules and motions within DPDPE cause fluctuations in the orientations of the rings relative to each other and with respect to the bilayer normal. The CSA has components within the plane of the ring and perpendicular to the plane, whereas all of the ^1H-^{13}C dipolar interaction vectors are within the plane. Consequently, the differences in predicted coordinates may be a result of how the two observables are averaged by the local fluctuations.

In the second approach to characterizing the arrangement of the rings, the observed dipolar couplings and CSAs for the two aromatic rings were found to be consistent with two of the three conformations of DPDPE present in the published crystal structure, MOL1 and MOL3 (Flippen-Anderson et al., 1994). The orientation of the molecular director through the MOL1 and MOL3 structures suggests that the hydrophobic Phe ring is directed into the bilayer, given that the hydrophilic Tyr ring is most likely directed outward toward the aqueous phase (Fig. 8).

Overall, these results suggest that the two aromatic rings are oriented with the plane of the ring tilted 15° ± 15° from the bilayer normal. This is similar to what was observed for the aromatic ring of pyridine (Henderson et al., 1994) and benzyl alcohol (Boden et al., 1988) adsorbed to the water/lipid interface.

Kimuri, Kunil and Fujiwara have proposed conformations for Met-enkephalin (Kimura et al., 1996) and the δ-active [D-Ala^2]- and inactive [L-Ala^2]-Met-enkephalins (Kimura et al., 1997) in cesium perfluorooctanoate liquid crystals, using ^1H-^1H dipolar couplings in pseudoenergy terms for molecular modeling. The published structures have the planes of the Tyr and Phe rings nearly parallel for the inactive [L-Ala^2]-Met-enkephalin (Kimura et al., 1997), whereas the two rings appear far from parallel for the δ-active [D-Ala^2]-Met-enkephalin (Kimura et al., 1997) and Met-enkephalin itself (Kimura et al., 1996). The relative orientations of the DPDPE Tyr and Phe rings of DHPC/DMPC are more similar to that for the inactive [L-Ala^2]-Met-enkephalin in the perfluorooctoanoate. This could be an indication that the membrane-bound conformations do not correlate with activity. However, there may be a real difference in peptide conformation when bound to the anionic perfluorooctanoate micelles versus the zwitterionic phospholipid micelles. Furthermore, it is very likely that peptide and micelle dynamics cause the orientations of the two rings to fluctuate with respect to each other and with respect to the micelle surface. The data analysis used here and in the Met-enkephalin studies implicitly assumes a static arrangement of the rings in the micelles. In the case of DPDPE, the orientations of the two rings were analyzed individually, with no reference to other parts of the molecule. In the Met-enkephalin studies, the analysis included ^1H-^1H couplings from several sites and energy minimization of the entire molecule with pseudoenergy contributions from the couplings (Kimura et al., 1996, 1997). Even if the peptides have similar conformations in the two types of micelles, the local fluctuations will manifest as distortions in the computed conformations, and the two approaches in analysis will differ in the nature of the distortions. One other source of discrepancy between the DPDPE results and those

for the Met-enkephalin derivatives is that contributions from the micelle order parameter (S) and fraction of peptide bound (f) were neglected in the latter (Kimura et al., 1996, 1997). Both the free and bound states will contribute to rotating frame Overhauser effect spectroscopy measurements, resulting in some average structure. The dipolar couplings only arise for peptide bound to the oriented micelles, but the set of molecular coordinates found to satisfy the relation between the experimental and theoretical couplings will depend on the actual magnitudes of the couplings, which are dependent on f and S.

In comparing the DPDPE results with those for the Met-enkephalin analogs, it is clear to us that structure-activity studies of peptides in membranes should be performed with a single type of membrane mimetic system and a common approach in data analysis. Unfortunately, there is no ideal approach. The perfluorooctanoate system has the advantage of virtually no spectral interference in the ^{1}H spectrum of the peptide, with great potential for providing many details about peptide conformation from the Overhauser effects and dipolar couplings measured in rotating frame Overhauser effect spectroscopy/magic angle spinning and magic angle spinning/near-magic angle spinning experiments. These data are readily incorporated as constraints in conventional molecular modeling studies (Kimura et al., 1996, 1997). The phospholipid micelles suffer from spectral interference with peptide resonances, which is compounded by the fact that an excess of lipid over peptide must be used to ensure a significant fraction of bound peptide. However, the phospholipids may be a more realistic membrane mimetic system. Moreover, it may not be necessary to determine all of the details of the peptide conformation to test the concept of whether the membrane-bound conformation correlates with activity. Characterization of the key pharmacophores in the membrane may be sufficient and much less demanding. This approach is being taken in an analysis of a series of δ- and μ-opiate analogs (Rinaldi, 1997).

The use of the Bruker AMX500 NMR for the assignments and support for FR was made possible by Bristol-Myers Squibb. This work was supported by National Institutes of Health grant 1 R15 GM51048-01.

REFERENCES

Aue, W. P., E. Bartholdi, and R. R. Ernst. 1976. Two-dimensional spectroscopy. Application to nuclear magnetic resonance. *J. Chem. Phys.* 64:2229–2234.

Bax, A., and S. Subramanian. 1986. Sensitivity-enhanced two-dimensional heteronuclear shift correlation NMR spectroscopy. *J. Magn. Reson.* 67:565–569.

Bax, A., and M. F. Summers. 1986. ^{1}H and ^{13}C assignments from sensitivity-enhanced detection of heteronuclear multiple-bond connectivity by 2D multiple quantum NMR. *J. Am. Chem. Soc.* 108:2093–2094.

Bechinger, B., and S. J. Opella. 1991. Flat coil probe for NMR spectroscopy of oriented membrane samples. *J. Magn. Reson.* 95:585–588.

Bechinger, B., M. Zasloff, and S. J. Opella. 1993. Structure and orientation of the antibiotic peptide magainin in membranes by solid-state nuclear magnetic resononce spectroscopy. *Protein Sci.* 2:2077–2084.

Boden, N., R. J. Bushby, P. F. Knowles, and F. Sixl. 1988. Partial molecular surface areas as a probe of chemical equilibria in lipid bilayers: anticooperative binding of benzyl alcohol to dimyristoylphosphatidylcholine. *Chem. Phys. Lett.* 145:315–320.

Cevc, G., and D. Marsh. 1987. Phospholipid Bilayers: Physical Principles and Models. John Wiley and Sons, New York.

Duncan, T. M. 1987. ^{13}C chemical shieldings in solids. *J. Phys. Chem. Ref. Data.* 16:125–151.

Flippen-Anderson, J. L., V. J. Hruby, N. Collins, C. George, and B. Cudney. 1994. X-ray structure of [D-Pen^2,D-Pen^5]enkephalin, a highly potent, δ opioid receptor-selective compound: comparisons with proposed solution structure. *J. Am. Chem. Soc.* 116:7523–7531.

Gibbs, S. J., C. S. Johnson. 1991. A PFG NMR experiment for accurate diffusion and flow studies in the presence of eddy currents. *J. Magn. Reson.* 93:395–402.

Graham, W. H., E. S. Carter II, and R. P. Hicks. 1992. Conformational analysis of Met enkephalin in both aqueous solution and in the presence of sodium dodecylsulfate micelles using multidimensional NMR and molecular modeling. *Biopolymers.* 32:1755–1764.

Gysin, B., and R. Schwyzer. 1984. Hydrophobic and electrostatic interactions between adrenocorticotropin-(1–24)-tetracosapeptide and lipid vesicles. Amphiphilic primary structures. *Biochemistry.* 23:1811–1818.

Henderson, J. M., R. M. Iannucci, and M. Petersheim. 1994. An NMR study of pyridine associated with DMPC liposomes and magnetically ordered DMPC-surfactant mixed micelles. *Biophys. J.* 67:238–249.

Herz, A. 1993. Handbook of Experimental Pharmacology. Springer-Verlag, Berlin, Heidelburg. 3–21.

Hicks, R. P., D. J. Beard, and J. K. Young. 1992. The interactions of neuropeptides with membrane model systems: a case study. *Biopolymers.* 32:85–96.

Howard, K. P., and J. H. Prestegard. 1995. Membrane and solution conformations of monogalactosyldiacylglycerol using NMR/molecular modeling methods. *J. Am. Chem. Soc.* 117:5031–5040.

Howard, K. P., and J. H. Prestegard. 1996. Conformation of sulfoquinovosyldiacylglycerol bound to a magnetically oriented membrane system. *Biophys. J.* 71:2573–2582.

Hu, W., and T. A. Cross. 1995. Tryptophan hydrogen bonding and electric dipole moments: functional roles in the gramicidin channel and implications for membrane proteins. *Biochemistry.* 34:14147–14155.

Hu, W., N. D. Lazo, and T. A. Cross. 1995. Tryptophan dynamics and structural refinement in a lipid bilayer environment: solid state NMR of the gramicidin channel. *Biochemistry.* 34:14138–14146.

Jelinek, R., A. Ramamoorthy, and S. J. Opella. 1995. High-resolution three-dimensional solid-state NMR spectroscopy of a uniformly ^{15}N-labeled protein. *J. Am. Chem. Soc.* 117:12348–12349.

Karslake, C., M. E. Piotto, Y. K. Pak, H. Weiner, and D. G. Gorenstein. 1990. 2D NMR and structural model for a mitochondrial signal peptide bound to a micelle. *Biochemistry.* 29:9872–9878.

Kimura, A., N. Kuni, and H. Fujiwara. 1996. Orientation and conformation of Met-enkephalin in a liquid crystal as studied by magic-angle- and near-magic-angle-spinning two-dimensional NMR spectroscopy. *J. Phys. Chem.* 100:14056–14061.

Kimura, A., N. Kuni, and H. Fujiwara. 1997. Conformation and orientation of Met-enkephalin analogues in a lyotropic liquid crystal studied by the magic-angle- and near-magic-angle-spinning two-dimensional methodology in nuclear magnetic resonance: relationships between activities and membrane-associated structures. *J. Am. Chem. Soc.* 119: 4719–4725.

Lee, K.-C., S. Huo, and T. A. Cross. 1995. Lipid-peptide interface: valine conformation and dynamics in the gramacidin channel. *Biochemistry.* 34:857–867.

Meiboom, S., and L. C. Snyder. 1971. Nuclear magnetic resonance spectra in liquid crystals and molecular structure. *Acc. Chem. Res.* 4:81–87.

Morris, K. F., and C. S. Johnson. 1993. Resolution of discrete and continuous molecular size distributions by means of diffusion-ordered 2D NMR spectroscopy. *J. Am. Chem. Soc.* 115:4291–4299.

Mosberg, H. I., R. Hurst, V. J. Hruby, K. Gee, H. I. Yamamura, J. J. Galligan, and T. F. Burks. 1983. Bis-penicillamine enkephalins possess highly improved specificity toward δ opioid receptors. *Proc. Natl. Acad. Sci. USA.* 80:5871–5874.

Murari, R., M. P. Murari, and W. J. Baumann. 1986. Sterol orientation in phosphatidylcholine liposomes as determined by deuterium NMR. *Biochemistry.* 25:1062–1067.

North, C. L., M. Barranger-Mathys, and D. S. Cafiso. 1995. Membrane orientation of the N-terminal segment of alamethicin determined by solid-state ^{15}N NMR. *Biophys. J.* 69:2392–2397.

Okada, A., K. Wakamatsu, T. Miyazawa, and T. Higashijima. 1994. Vesicle-bound conformation of melittin: transferred nuclear Overhauser enhancement analysis in the presence of perdeuterated phosphatidylcholine vesicles. *Biochemistry.* 33:9438–9446.

Opella, S. J. 1994. Solid-state NMR structural studies of proteins. *Annu. Rev. Phys. Chem.* 45:659–683.

Opella, S. J., Y. Kim, and P. McDonnell. 1994. Experimental nuclear magnetic resonance studies of membrane proteins. *Methods Enzymol.* 239:536–560.

Pausak, S. J., J. S. Tegenfeldt, and J. Waugh. 1974. ^{13}C chemical shielding tensors in polyalkylbenzenes. *J. Phys. Chem.* 61:1338–1344.

Prosser, R. S., S. A. Hunt, J. A. DiNatale, and R. R. Vold. 1996. Magnetically aligned membrane model systems with positive order parameter: switching the sign of S_{zz} with paramagnetic ions. *J. Am. Chem. Soc.* 118:269–270.

Reynaud, J. A., J. P. Grivet, D. Sy, and Y. Trudelle. 1993. Interactions of basic amphiphilic peptides with dimyristoylphosphatidylcholine small unilamellar vesicles: optical, NMR and electron microscopy studies and conformational calculations. *Biochemistry.* 32:4997–5008.

Rinaldi, F. 1997. On the conformation of opioid peptides bound to phospholipid micelles. Ph.D. dissertation, Seton Hall University, South Orange, NJ.

Sanders, C. R., II. 1993. Solid state ^{13}C NMR of unlabeled phosphatidylcholine bilayers: spectral assignments and measurements of carbon-phosphorous dipolar couplings and ^{13}C chemical shift anisotropies. *Biophys. J.* 64:171–181.

Sanders, C. R., II, and G. C. Landis. 1995. Reconstitution of membrane proteins into lipid-rich bilayered mixed micelles for NMR studies. *Biochemistry.* 34:4030–4040.

Sanders, C. R., II, and J. H. Prestegard. 1990. Magnetically oriented phospholipid bilayers containing small amounts of a bile salt analogue, CHAPSO. *Biophys. J.* 58:447–460.

Sanders, C. R., II, and J. H. Prestegard. 1991. Orientation and dynamics of β-dodecyl glucopyranoside in phospholipid bilayers by oriented sample NMR and order matrix analysis. *J. Am. Chem. Soc.* 113:1987–1996.

Sanders, C. R., II, and J. H. Prestegard. 1992. Headgroup orientations of alkyl glycosides at a lipid bilayer interface. *J. Am. Chem. Soc.* 114: 7096–7107.

Sanders, C. R., II, J. E. Schaff, and J. H. Prestegard. 1993. Orientational behavior of phosphatidylcholine bilayers in the presence of aromatic amphiphiles and a magnetic field. *Biophys J.* 64:1069–1080.

Sargent, D. F., and R. Schwyzer. 1986. Membrane lipid phase as catalyst for peptide-receptor interactions. *Proc. Natl. Acad. Sci. USA.* 83: 5774–5778.

Schiller, P. W. 1984. Conformational analysis of enkephalins and conformation-activity relationships. *In* The Peptides. Academic Press, San Diego. 219–267.

Schwyzer, R. 1977. ACTH: a short introductory review. *Ann. N.Y. Acad. Sci.* 297:3–26.

Schwyzer, R. 1986. Molecular mechanism of opioid receptor selection. *Biochemistry.* 25:6335–6342.

Smith, P. E., L. X. Dang, and B. M. Pettitt. 1991. Simulation of the structure and dynamics of bis(penicillamine) enkephalin zwitterion. *J. Am. Chem. Soc.* 113:67–73.

Tausk, R. J. M., J. Van Esch, J. Karmigglet, G. Voordouw, and J. T. G. Overbeek. 1974. Physical chemical studies of short-chain lecithin homologues. II. Micellar weights of dihexanoyl- and diheptanoyllecithin. *Biophys. Chem.* 1:184–203.

Tourwe, D., K. Verschueren, A. Frycia, P. Davis, F. Porreca, V. J. Hruby, G. Toth, H. Jaspers, P. Verheyden, and G. Van Binst. 1996. Conformational restriction of Tyr and Phe side chains in opioid peptides: information about preferred and bioactive side-chain topology. *Biopolymers.* 38:1–12.

Weast, R. C. 1983. CRC Handbook of Chemistry and Physics. F-171.

Wingard, L. B., Jr., T. M. Brody, J. Larner, and A. Scharwz. 1991. Human Pharmacology: Molecular to Clinical. Mosby-Year Book, St. Louis. 385–395.

Wooley, G. A, and C. M. Deber. 1987. Peptides in membranes: lipid-induced secondary structure of substance P. *Biopolymers.* 26: S109–S121.